Thomas-Fermi-Poisson theory of screening for laterally confined and unconfined two-dimensional electron systems in strong magnetic fields

A. Siddiki and Rolf R. Gerhardts
Max-Planck-Institut für Festkörperforschung, Heisenbergstrasse 1, D-70569 Stuttgart, Germany
(Received 9 April 2003; published 16 September 2003)

We examine within the self-consistent Thomas-Fermi-Poisson approach the low-temperature screening properties of a two-dimensional electron gas (2DEG) subjected to strong perpendicular magnetic fields. Numerical results for the unconfined 2DEG are compared with those for a simplified Hall-bar geometry realized by two different confinement models. It is shown that in the strongly nonlinear-screening limit of zero temperature the total variation of the screened potential is related by simple analytical expressions to the amplitude of an applied harmonic modulation potential and to the strength of the magnetic field.

DOI: 10.1103/PhysRevB.68.125315 PACS number(s): 73.20.−r, 73.50.Jt, 71.70.Di

I. INTRODUCTION

A two-dimensional electron gas (2DEG) in a strong perpendicular magnetic field has unusual low-temperature screening properties,[1,2] since the highly degenerate Landau-quantized energy levels lead to a strong variation of the thermodynamic density of states (TDOS) with varying strength of the magnetic field, i.e., with varying filling factor ν of the Landau levels (LL's). If a LL is close to half filled, the TDOS is very high (inversely proportional to the temperature T), and static potential fluctuations are nearly perfectly screened. We will consider only spin-degenerate 2DEG's, so that this happens if the value of ν is close to an odd integer, while at even-integer ν the Fermi energy lies in the gap between two adjacent LL's and a spatial redistribution of electrons and, therefore, a screening of (weak) potential fluctuations is impossible. In an inhomogeneous 2DEG with sufficiently strong long-range density fluctuations, screening effects lead to quasimetallic (so-called ''compressible'') regions with high TDOS, in which screening is nearly perfect and a LL is ''pinned'' to the Fermi energy, and to insulatorlike ''incompressible'' regions, which separate adjacent compressible regions. In the incompressible regions the Fermi energy falls into the gap between two LL's and the electron density $n_{\rm el}(\mathbf{r})$ is constant (even-integer filling factor), while in the compressible region $n_{\rm el}(\mathbf{r})$ adjusts itself so that the self-consistent electrostatic potential energy $V(\mathbf{r})$ of an electron differs from the Fermi energy (more precisely the electrochemical potential $\mu^\star$) by a Landau energy $\hbar\omega_c(n+1/2)$, where $\omega_c=eB/m$ is the cyclotron frequency in the magnetic field B. As a consequence, $V(\mathbf{r})$ becomes nearly constant within a compressible region and differs by integer multiples of $\hbar\omega_c$ between different compressible regions. Landau level pinning and the interplay of compressible and incompressible regions lead to strongly nonlinear screening effects. This screening scenario was established some time ago[1,2] and was applied, e.g., to calculate, at zero temperature, the electronic DOS (Ref. 3) and transport[4,5] through 2DEG's in smooth periodic and random potentials. The explanation[6,7] of several experimental results, e.g., on quantum Hall devices under high currents close to the breakdown of the quantized Hall effect[8,9] relies also on these ideas. A systematic investigation of these interesting nonlinear screening effects is, however, apparently not available in the literature.

Models for half-space and Hall-bar geometries with planar charge distributions have been proposed that allow closed solutions of Poisson's equation (i.e., calculation of the potential for a given electron density), and estimates of position and widths of the incompressible strips have been given.[10,11] By adding the nonlinear Thomas-Fermi approximation for the calculation of the electron density from the potential, that work was extended to a self-consistent approach, which allows us to calculate both electron density and electrostatic potential for arbitrary temperature.[12,13] This approach, which we will employ in the following, shows that the existence and width of incompressible strips depend sensitively on temperature and allows us to calculate their position and width for given background charges without additional assumptions.

The purpose of the present work is a systematic investigation of the nonlinear low-temperature screening of harmonic electrostatic potential modulations in laterally confined and unconfined 2DEG's subjected to a quantizing perpendicular magnetic field. We will demonstrate that in general edge effects do not qualitatively change the screening properties of the 2DEG, even if the sample width is not much larger than the period of the imposed potential modulation. There are, however, peculiar differences between confined and unconfined 2DEG's in situations in which the latter have no states near the Fermi energy. To understand this in detail, we first discuss the screening of a potential modulation imposed on a homogeneous 2DEG (Sec. II) and then consider, for two different boundary models, edge effects on screening in Hall-bar geometries (Sec. III).

We will assume the 2DEG to be located in the plane $z=0$ with a (surface) number density $n_{\rm el}(x)$ and consider only situations with translation invariance in the y direction. The (Hartree) contribution $V_H(x)$ to the potential energy of an electron caused by the total charge density of the 2DEG can be written as[13]

$$V_H(x)=\frac{2e^2}{\kappa}\int_{x_l}^{x_r}dx'K(x,x')n_{\rm el}(x'), \tag{1}$$

where $-e$ is the electron charge, $\overline{\kappa}$ an average background dielectric constant,[13] and the kernel $K(x,x')$ describes the solution of Poisson's equation with appropriate boundary conditions at x_l and x_r. The electron density in turn is calculated in the Thomas-Fermi approximation[13] (TFA)

$$n_{\rm el}(x)=\int dE D(E) f([E+V(x)-\mu^\star]/k_BT), \qquad (2)$$

with $D(E)$ the relevant (single-particle) density of states, $f(\epsilon)=[1+e^{\epsilon}]^{-1}$ the Fermi function, and $\mu^\star$ the electrochemical potential and with $V(x)=V_{\rm ext}(x)+V_H(x)$ the total potential energy of an electron, which differs from $V_H(x)$ by the contribution due to external charges, e.g., a homogeneous positively charged background and a charge distribution creating a periodic modulation potential. The local (but nonlinear) TFA is much simpler than the corresponding quantum mechanical calculation and expected to yield essentially the same results if $V(x)$ varies slowly in space, i.e., on a length scale much larger than typical quantum lengths such as the extent of wave functions or the Fermi wavelength.

II. HOMOGENEOUS 2DEG

We start with a homogeneous 2DEG described by the DOS $D_0(E)=D_0\theta(E)$, with $D_0=m/(\pi\hbar^2)$, for $B=0$, and by the Landau DOS

$$D_B(E)=\frac{1}{\pi l_m^2}\sum_{n=0}^{\infty}\delta(E-E_n),\quad E_n=\hbar\omega_c(n+1/2) \qquad (3)$$

for finite B. The effective mass of an electron is denoted by m, the magnetic length by $l_m=\sqrt{\hbar/(m\omega_c)}$. In both cases we assume spin degeneracy and neglect collision broadening effects. The constant electron density $\overline{n_{\rm el}}$ is given by Eq. (2) with $\overline{n_{\rm el}}=n_{\rm el}(x)$, $V(x)\equiv 0$, and $\mu^\star=\mu$ the chemical potential. For these simple models the energy integral in Eq. (2) is readily carried out. We tacitly assume that the electron charges are neutralized by a homogeneous background of positive charges.

A. Kernel for periodic modulation

We now add a periodic external modulation described by a potential energy $V_{\rm ext}(x)=V_{\rm ext}(x+a)$. The 2DEG will respond with a density modulation and a Hartree potential of the same period a. To exploit the periodicity, we expand density and potentials into Fourier series according to

$$V(x)=\sum_q V^q e^{iqx},\quad V^q=\int_{-a/2}^{a/2}\frac{dx}{a}e^{-iqx}V(x), \qquad (4)$$

with $q=2\pi n/a$ and integer n. To maintain charge neutrality, we require $n_{\rm el}^0=\overline{n_{\rm el}}$ in any case. With the boundary conditions $V_H(x,z)\to 0$ for $|z|\to\infty$, Poisson's equation yields (see, e.g., Ref. 14)

$$V_H^q(z)=(2\pi e^2/\overline{\kappa}|q|)e^{-|qz|}n_{\rm el}^q \qquad (5)$$

as response to the density fluctuation $n_{\rm el}^q$. Summing over harmonics (for $q\neq 0$),[15] we obtain $V_H(x,z=0)$ from Eq. (1) with $-x_l=x_r=a/2$ and the kernel

$$K(x,x')=-\ln\left|2\sin\frac{\pi}{a}(x-x')\right|. \qquad (6)$$

B. Breakdown of linear screening

1. Zero magnetic field

In the limit $B=0$, $T\to 0$ and with $E_F=\mu^\star(B=0,T=0)$, Eq. (2) reduces to

$$n_{\rm el}(x)=D_0(E_F-V(x))\theta(E_F-V(x)), \qquad (7)$$

which is a linear relation between $V(x)$ and $n_{\rm el}(x)$ for $V(x)<E_F$. With Eq. (5) we find for a harmonic potential modulation $V_{\rm ext}(x)=V_{\rm ext}^q\cos qx$ a harmonic density modulation $\delta n_{\rm el}(x)=n_{\rm el}^q\cos qx$ and the self-consistent (''screened'') potential $V(x)=V^q\cos qx$ with

$$V^q=V_{\rm ext}^q/\epsilon(q),\quad \epsilon(q)=1+Q_0/|q|. \qquad (8)$$

The dielectric function $\epsilon(q)$ can be expressed in terms of the effective Bohr radius $a_{\rm B}^\star=\overline{\kappa}\hbar^2/(me^2)$ (for GaAs $a_{\rm B}^\star=9.8$ nm), since $Q_0=2\pi e^2 D_0/\overline{\kappa}=2/a_{\rm B}^\star$.[1,16] With $q=2\pi/a$, the screening strength is thus determined by the dimensionless parameter

$$\alpha=\pi a_{\rm B}^\star/a. \qquad (9)$$

We will assume $\alpha\ll 1$, i.e., $\epsilon(q)=1+1/\alpha\gg 1$, so that the TFA is valid for $B\gtrsim 1$ T, i.e., $l_m\lesssim 30$ nm. Since in the linear screening regime the minimum value of the electron density is $n_{\rm el}(0)=D_0(E_F-V^q)$, linear screening breaks down if the modulation strength becomes so large that $V^q\geqslant E_F$, i.e., for $V_{\rm ext}^q\geqslant\epsilon(q)E_F$. For larger modulation amplitude the redistribution of electrons is hindered: while the electron density at the minimum of $V_{\rm ext}(x)$ still increases, the electron density at the maximum of $V_{\rm ext}(x)$ cannot decrease further. Instead the density minimum becomes broader. This means that the electrons are depleted from strips along the maxima of $V_{\rm ext}(x)$ and the 2DEG breaks off into a system of parallel quasi-one-dimensional ribbons. Thus, the imposed harmonic modulation potential $V_{\rm ext}(x)$ now leads to an anharmonic density distribution and, therefore, an anharmonic screened potential.[17] Mathematically, Eq. (1) with (6) and Eq. (7) now represents a nonlinear integral equation that must be solved numerically. In Fig. 1 we plot the total variance $\mathrm{Var}[V]=V(0)-V(a/2)$ as a function of the amplitude $V_{\rm ext}^q\equiv V_0$ of the imposed modulation potential for several values of the magnetic field. The result for $B=0$ and $T=0$ is shown as a thick solid line. In the linear screening regime, $\mathrm{Var}[V]\equiv 2V^q=2V_0/\epsilon(q)$. As linear screening breaks down, a kink appears in the line and the variance increases much faster than in the linear regime. With increasing temperature this kink is rounded off, while the $\mathrm{Var}[V]$-vs-V_0 curve as a whole is not much affected (shown for $k_BT/E_F=0.04$ by the open circles in Fig. 1). Here and in the following we measure

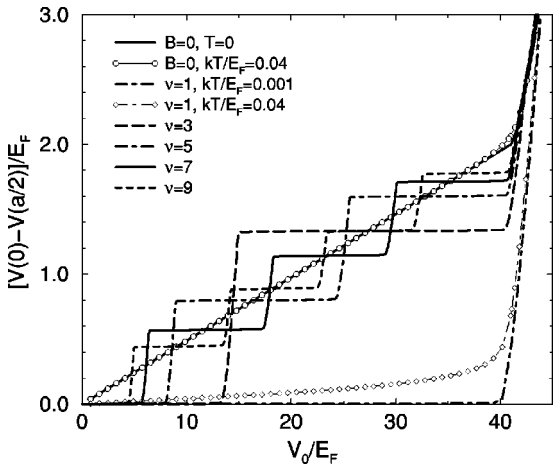

FIG. 1. Variance of the screened potential vs amplitude of the harmonic potential modulation imposed on a spin-degenerate homogeneous 2DEG with a half-filled Landau level, for several odd-integer values of the filling factor. Default temperature $k_BT/E_F=0.001$, $\epsilon(q)=41$.

energies in units of the Fermi energy $E_F=\overline{n}_{\rm el}/D_0$ (for GaAs with $\overline{n}_{\rm el}\approx 3\times 10^{11}$ cm^{-2}, $E_F\approx 10$ meV), and we keep the mean electron density $\overline{n}_{\rm el}$, and thus E_F, constant. We will focus in the following on the regime $V_0\lesssim\epsilon(q)E_F$, where screening is linear in the limit $B=0$, $T=0$.

2. Half-filled Landau levels

With the Landau DOS [see Eq. (3)] and the definition of a position-dependent chemical potential, $\mu(x)=\mu^\star-V(x)$, Eq. (2) yields

$$n_{\rm el}(x)=\hbar\omega_c D_0\sum_n f(E_n-\mu(x)). \tag{10}$$

We may also write the argument of the Fermi function as $E_n(x)-\mu^\star$ and interpret $E_n(x)=E_n+V(x)$ as position-dependent Landau energies, which is correct if the Thomas-Fermi approximation holds. It will be useful to define, in addition to the average LL filling factor $\overline{\nu}=2\pi l_m^2\overline{n}_{\rm el}$, a local filling factor $\nu(x)=2\pi l_m^2 n_{\rm el}(x)$.

For $k_BT\ll\hbar\omega_c$ and a homogeneous 2DEG with partly filled nth Landau level, $\mu\sim E_n$, $\overline{\nu}=2n+\nu_n$, where $\nu_n\approx 2f(E_n-\mu)$ is the filling factor of the nth Landau level, the TDOS is[1]

$$D_T(\mu;B)\equiv\frac{\partial\overline{n}_{\rm el}}{\partial\mu}=\frac{\hbar\omega_c}{k_BT}\frac{\nu_n}{2}\left(1-\frac{\nu_n}{2}\right)D_0, \tag{11}$$

which is peaked around $\mu=E_n$ with a maximum value $\hbar\omega_c D_0/(4k_BT)$ and a width of order k_BT [a crude approximation is $D_T(\mu;B)\approx(\hbar\omega_c D_0/4k_BT)\,\theta(2k_BT-|E_n-\mu|)$]. Linearizing Eq. (10) with respect to the screened potential $V(x)$, we obtain the Eq. (8) with Q_0 replaced by $Q_B=Q_0D_T(\mu;B)/D_0\gg Q_0$,

$$\epsilon(q;B)=1+\frac{\hbar\omega_c}{k_BT}\frac{\nu_n}{2}\left(1-\frac{\nu_n}{2}\right)\frac{Q_0}{|q|}. \tag{12}$$

For exactly half filling, $\mu=E_n$, this is a rather good approximation, as can be seen from Fig. 1, which shows numerical results for $\overline{\nu}=\nu_0=1$ ($n=0$) at two different temperatures (two lowest curves at $V_0/E_F>15$). We see that the screening at finite magnetic field depends much stronger on temperature than at $B=0$. The linear approximation breaks down if the amplitude of the screened potential becomes of the order $2k_BT$.

This yields, in the limit of low temperatures and for $\nu_n=1$, the estimate for the linear screening regime,

$$\frac{V_{\rm ext}^q}{E_F}\lesssim\epsilon(q;B)\frac{2k_BT}{E_F}\approx\frac{\epsilon(q)}{\overline{\nu}}, \tag{13}$$

with $\epsilon(q)=\epsilon(q;B=0)=1+1/\alpha$. For a larger modulation the redistribution of electrons within the considered LL is not efficient enough to screen the imposed modulation potential, and similar to the $B=0$ case, the variance of the screened potential increases much stronger than in the linear regime. In Fig. 1 we show low-temperature ($k_BT/E_F=0.001$) results for odd-integer $\overline{\nu}$ values, calculated numerically from Eqs. (1), (6), and (10). For this temperature, the linear increase of the screened potential with the applied modulation amplitude V_0 is not resolved on the scale of Fig. 1. However the rapid increase of the variance of the screened potential at $V_0/E_F\sim\epsilon(q)/\overline{\nu}$ is clearly seen for the indicated $\overline{\nu}$ values.

For $\overline{\nu}=1$ the situation is very similar to the $B=0$ case, apart from the fact that screening in the linear regime is much stronger (''perfect screening,'' ''pinning of lowest LL to Fermi level'') due to the higher DOS. For $\overline{\nu}>1$ new phenomena occur, which we will now discuss.

C. Emergence of incompressible strips

1. Odd-integer filling factor $\overline{\nu}$

We start with filling factor $\overline{\nu}=3$ and investigate the changes of the electron density (Fig. 2) and of the total potential (Fig. 3) with increasing amplitude V_0 of the imposed modulation $V_{\rm ext}(x)=V_0\cos qx$, giving explicit results for the six typical V_0 values indicated by open circles in Fig. 2.

For $V_0=11E_F$, close to the breakdown of linear screening (case 1), the density is strongly modulated (see thin line in lower inset of Fig. 2), but the modulation appears still cosine like. The potential is so effectively screened that the second-lowest LL ($n=1$) is pinned (within a few k_BT) to the Fermi energy [see Fig. 3(1)]. For case 2, $V_0=13.7E_F$, the total potential has developed locally confined maxima and minima, while it remains rather flat in between [Fig. 3(2)]. Near these extrema $|E_1(x)-\mu^\star|$ becomes so large that the LL $n=1$ is completely occupied (near $x=a/2$) or empty (near $x=0$), and incompressible strips with local filling factors $\nu(x)=4$ and $\nu(x)=2$ develop near the potential minima and maxima, respectively [see thick solid line in the lower inset of Fig. 2 and Fig. 3(2)]. Increasing the modulation to

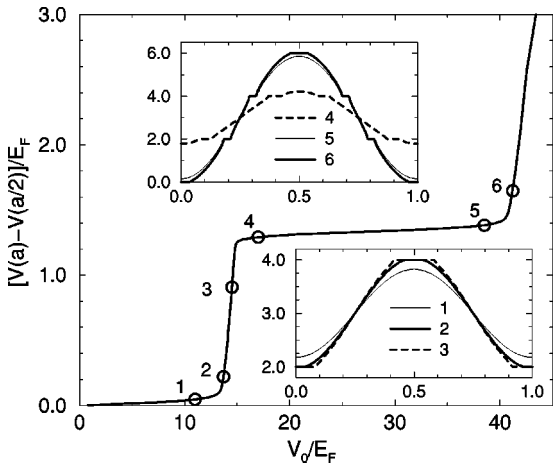

FIG. 2. Variance of the total potential vs V_0, for average filling factor $\bar{\nu}=3$. The insets show the local filling factor $\nu(x)$ in one modulation period ($0\leqslant x/a\leqslant 1$) for the six V_0 values indicated by circles. Parameters: $k_BT/E_F=0.01$, $\epsilon(q)=41$, $q=2\pi/a$.

$V_0=14.5E_F$ (case 3) leads to more pronounced local extrema and broader incompressible strips, but does not change the situation qualitatively. The overall change of the density distribution is rather small (see lower inset of Fig. 2), indicating poor screening. Indeed the slope of the Var$[V]$-vs-V_0 curve in this regime is $\Delta\mathrm{Var}/\Delta V_0\approx 1$, i.e., only slightly smaller than in the absence of any screening, which would yield $\Delta\mathrm{Var}/\Delta V_0=2$. We note that in the incompressible strips the local filling factor (i.e., the density) is constant, while in the pinning regions, i.e., the compressible strips, the screened potential still has a finite slope, proportional to k_BT.[12]

As V_0 increases further to case 4 ($V_0=17E_F$), the modulation becomes so strong that the maximum of the lowest LL, $E_0(0)$, and the minimum of the lowest unoccupied LL, $E_2(a/2)$, reach the Fermi level $\mu^\star$ (to within k_BT). Then thermal population of the higher LL ($n=2$ near $x=a/2$) and depletion of the lower LL ($n=0$ near $x=0$) starts and compressible strips emerge in the center of each incompressible strip [see dashed line in the upper inset of Fig. 2 and Fig. 3(4)]. Further increase of V_0 up to $V_0=38.5E_F$ (case 5) widens the compressible strips and leads to a strong increase of the density modulation due to a redistribution of electrons from the $n=0$ to the $n=2$ LL. This results in a strong screening, similar to that in the linear screening regime at weak modulation, and, apart from a weak increase with a slope proportional to k_BT, the variance Var$[V]=V(0)-V(a/2)$ remains constant at the value Var$[V]=\mu^\star-E_0(0)-[\mu^\star-E_2(a/2)]=2\hbar\omega_c$. This plateau behavior of the Var$[V]$-vs-V_0 curve is obviously an immediate consequence of the pinning of LLs to the Fermi level, i.e., of the nearly perfect screening.

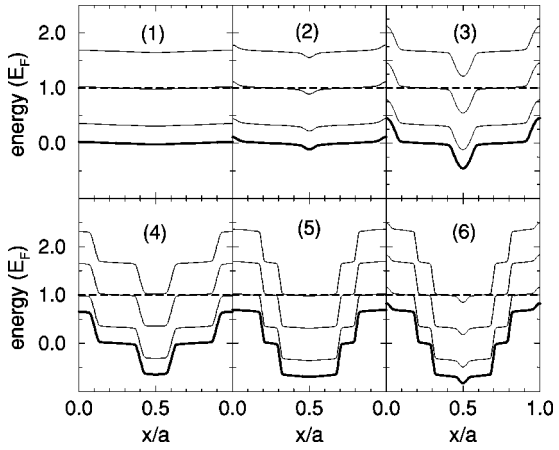

FIG. 3. Total potential (thick solid lines) and the three lowest of the corresponding Landau levels (thin solid lines) together with the electrochemical potential (thick dashed lines) for the six V_0 values indicated in Fig. 2. Parameters as in that figure.

In case 5 we reach a situation in which the lowest ($n=0$) LL is nearly empty at the potential maximum and the higher ($n=2$) LL nearly full at the potential minimum. In case 6 ($V_0=41.2E_F$) the total potential again develops local extrema, similar to the situation depicted in Fig. 3(2). But now the incompressible strip created at the potential maximum is due to the depopulation of the lowest LL, i.e., due to vanishing electron density. With further increasing V_0 the depletion regions become wider and the density near the potential minima increases, but screening remains much poorer than in the plateau region.

We see from Fig. 2 that the global appearance of the density modulation, apart from a fine structure related to the incompressible strips, is more or less cosine like. We will use this finding for a rough estimate of the plateau width of the Var$[V]$-vs-V_0 curves. First we conclude from the cosinelike form of the induced density variation that in the high-screening plateau region, along with Eqs. (5) and (8), the first relation of Eq. (13) holds qualitatively and relates the changes δV of the total potential to the changes δV_0 of the externally applied potential by $\delta V\sim\epsilon(q;B)\,\delta V_0$. For $Q/|q|\gg 1$, this yields for the change of the variance Var$[V]$ across the plateau of width ΔV_0:

$$\Delta\mathrm{Var}[V]\sim\frac{8k_BT}{\hbar\omega_c\epsilon(q)}\Delta V_0, \tag{14}$$

i.e., an estimate for the slope of the Var$[V]$-vs-V_0 curve in the plateau region. Since the modulation induces density changes δn_{el} mainly within the compressible regions of high TDOS, we estimate $\delta n_{\mathrm{el}}\sim -D_T(\mu;B)\,\delta V\sim -(\hbar\omega_c/4k_BT)D_0\,\delta V$ (which holds for $\nu_n=1$ and $|\delta V|\lesssim 2k_BT$). In terms of $\delta\nu=2\pi l_m^2\delta n_{\mathrm{el}}$ this yields $\delta V\sim 2k_BT\,\delta\nu$, and together with Eq. (14) the relation

$$\frac{\Delta V_0}{E_F}\sim\frac{\epsilon(q)}{2\bar{\nu}}\Delta\mathrm{Var}[\nu] \tag{15}$$

between the plateau width ΔV_0 and the change of the filling factor variance Var$[\nu]=\nu(a/2)-\nu(0)$ (defined at fixed V_0) across the plateau. This criterion applies also to the small-V_0 linear-screening regime, in which $\nu(x)$ varies within the same LL, with Var$[\nu]$ increasing from 0 to 2, i.e., $\Delta\mathrm{Var}[\nu]=2$ [see Eq. (13)]. The resulting width of the linear-screening regime, $\Delta V_0/E_F\approx\epsilon(q)/\bar{\nu}$, describes the numerical results of Fig. 1 for odd-integer $\bar{\nu}=2n+1$ quite well.

From the discussion of Figs. 2 and 3 we expect that, for $n>0$, the linear regime of the $\mathrm{Var}[V](V_0)$ curve is terminated by a step of height $2\hbar\omega_c=4E_F/\bar{\nu}$, which is followed by a plateau. While V_0 sweeps through the plateau, in addition to the LL with index n the two LL's with indices $n-1$ and $n+1$ are locally pinned to the Fermi level and lead to a total change $\Delta\mathrm{Var}[\nu]=4$ (for $\bar{\nu}=3$ from $\mathrm{Var}[\nu]=\nu(a/2)-\nu(0)=2$ on the left side to $\mathrm{Var}[\nu]=6$ on the right side of the plateau, as seen from the upper inset of Fig. 2). This yields the plateau width $\Delta V_0/E_F\approx 2\epsilon(q)/\bar{\nu}$. If $n-1=0$, the plateau will be followed by the breakdown regime. If $n-1>0$, the plateau will be followed by a further step of the same height to a plateau of the same width.

To summarize: at very low temperatures and odd-integer filling factors $\bar{\nu}=2n+1$, the variance $\mathrm{Var}[V]$ of the screened potential as function of the imposed modulation amplitude V_0 shows a linear screening regime for $V_0\lesssim\epsilon(q)E_F/\bar{\nu}$ which is followed by n successive steps of height $2\hbar\omega_c=4E_F/\bar{\nu}$ and width $\Delta V_0\approx 2\epsilon(q)E_F/\bar{\nu}$. The plateau of the nth step ends at the breakdown of the 2DEG into a pattern of isolated 1D systems, which leads to poor screening and is indicated in the $\mathrm{Var}[V](V_0)$ curve by a slope of order unity. At finite temperature, the plateaus assume finite positive slopes, which are estimated from Eq. (14) as $\Delta\mathrm{Var}[V]/\Delta V_0\approx 4\bar{\nu}k_BT/[\epsilon(q)E_F]$. These results, which describe the content of the numerically calculated Figs. 1–3 very well, depend, of course, on the high symmetry of the situations considered so far.

2. Even-integer filling factor $\bar{\nu}$

Another situation of high symmetry is that of an even-integer filling factor $\bar{\nu}=2n+2$, where n is the index of the highest occupied LL and the Fermi energy $E_F=\hbar\omega_c(n+1)$ lies in the middle between two adjacent LL's. According to Eqs. (13) and (12), the linear-screening regime shrinks to zero, since $\nu_n=2$. Thus, at very low temperature ($k_BT\ll\hbar\omega_c/2$) a weak modulation $V_{\mathrm{ext}}(x)=V_0\cos qx$ will not be screened, i.e., the local filling factor will be independent of the modulation, $\nu(x)\equiv\bar{\nu}$, and the total potential will equal the external one, with variance $\mathrm{Var}[V](V_0)=2V_0$. This situation changes when the modulation potential becomes so large that $|V_0-\hbar\omega_c/2|\sim k_BT$; i.e., the maximum energy $E_n(0)$ of the highest occupied and the minimum energy $E_{n+1}(a/2)$ of the lowest unoccupied LL approach the Fermi energy. Then, with increasing V_0 the LL n is depleted near $x=0$ while the LL $n+1$ is populated near $x=a/2$, forming compressible strips with local filling factors $\nu(x)<\bar{\nu}$ and $\nu(x)>\bar{\nu}$, respectively.

This is demonstrated in the inset of Fig. 4, which shows the local filling factor $\nu(x)$ for $k_BT/E_F=0.001$ and the average filling factor $\bar{\nu}=2$, i.e., $\hbar\omega_c=E_F$, and for the modulation strengths V_0 indicated by circles in the main figure. For $V_0/E_F=0.45$ in the nonscreening region the deviation $[\nu(x)-\bar{\nu}]$ is practically zero (numerically $<10^{-6}$), while for $V_0/E_F=0.6$ it is finite, although small (in the inset enhanced by a factor of 20), with narrow compressible strips.

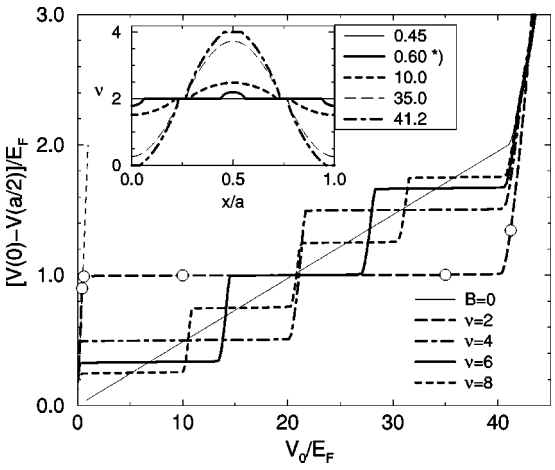

FIG. 4. As in Fig. 1 but for even-integer values of the (average) filling factor ($k_BT/E_F=0.001$, $\epsilon(q)=41$). The thin solid line indicates the result for $B=0$, $T=0$; the thin dashed line has slope 2. The inset shows the local filling factor $\nu(x)$ in one modulation period for average filling $\bar{\nu}=2$ and the five values of V_0 indicated by circles in the main figure. *) For $V_0/E_F=0.60$ the deviation $[\nu(x)-2]$ is enhanced by a factor of 20.

Between $V_0/E_F=0.5$ and $V_0/E_F\approx 41$ the width of the compressible strips and the deviation $[\nu(x)-\bar{\nu}]$ increase continuously, while the variance $\mathrm{Var}[V]\approx\hbar\omega_c=E_F$ remains constant. Since screening is due to the redistribution of electrons at the Fermi energy, i.e., to electrons in the compressible strips where the TDOS is large, we may again use Eq. (15) to estimate the plateau width. At the beginning of the first plateau the filling factor is constant, $\nu(x)\equiv\bar{\nu}$, i.e., $\mathrm{Var}[\nu]=0$. At the end of the plateau, the LL n is depleted at the potential maximum, $\nu(0)=\bar{\nu}-2$, and at the potential minimum the LL $n+1$ is full, $\nu(a/2)=\bar{\nu}+2$, i.e., $\mathrm{Var}[\nu]=4$. Thus, we have to use Eq. (15) with $\Delta\mathrm{Var}[\nu]=4$ and obtain for the plateau width $\Delta V_0\sim 2\epsilon(q)E_F/\bar{\nu}$.

This estimate is obviously in good agreement with the numerical calculations presented in Fig. 4. For filling factor $\bar{\nu}=2$, i.e., $n=0$, the first plateau ends at the transition to the poor-screening breakdown regime, since then the lowest LL $n=0$ is completely depleted at the potential maxima (thick dash-dotted line in the inset of Fig. 4). For $\bar{\nu}=2n+2$ with $n>0$ a behavior similar to that discussed in Fig. 3 occurs. As V_0 increases slightly beyond the plateau regime, a narrow local maximum of $V(x)$ develops near $x=0$, accompanied by an incompressible strip of filling $\nu(x)=2n$ due to the local depletion of the LL n. Simultaneously, a narrow local minimum of $V(x)$ develops near $x=a/2$, accompanied by an incompressible strip of filling $\nu(x)=2n+4$ due to the local occupation of the LL $n+1$. Then, in a narrow V_0 interval these new extrema become more pronounced and the accompanied incompressible strips widen a little. However, the accompanied density change is small, resulting in a poor screening and a rapid increase of the $\mathrm{Var}[V](V_0)$ curve. This interval ends when the new maximum $E_{n-1}(0)$ of the Landau level $n-1$ and the new minimum $E_{n+2}(a/2)$ of the LL $n+2$ come close to the Fermi level (within a few k_BT).

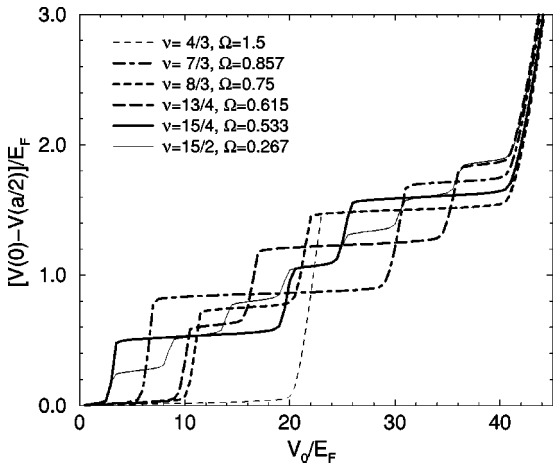

FIG. 5. As in Fig. 1 but for some noninteger values of the (average) filling factor and for higher temperature, $k_BT/E_F=0.01$ [$\epsilon(q)=41$].

Then, with further increasing V_0, new compressible strips open at the locations of the potential extrema, and a plateau region of the Var$[V](V_0)$ curve with ''perfect'' screening sets in. We thus again find a step behavior like in Fig. 1 with step height $\Delta\mathrm{Var}[V]=2\hbar\omega_c=4E_F/\overline{\nu}$. During the V_0 sweep through the corresponding plateau, the LL $n-1$ will be depleted near x_0, while the LL $n+2$ is occupied near $x=a/2$. Thus, we can estimate the plateau width from Eq. (15) with $\Delta\mathrm{Var}[\nu]=4$. The last plateau is the one corresponding to the local depletion of the $n=0$ LL.

In summary, for $\overline{\nu}=2n+2$ and very low temperature, the Var$[V](V_0)$ curve shows a linear increase with slope 2 for $0\leqslant V_0\leqslant E_F/\overline{\nu}$, followed by a plateau of height $\hbar\omega_c=2E_F/\overline{\nu}$ and width $\Delta V_0\sim 2\epsilon(q)E_F/\overline{\nu}$. This plateau is followed by n steps of height $2\hbar\omega_c$ and approximately the same width ΔV_0. The plateau of the last step is followed by the breakdown regime.

3. Noninteger filling factor $\overline{\nu}$

In Fig. 5 we show Var$[V](V_0)$ curves for a few noninteger values of the average filling factor $\overline{\nu}=2n+\nu_n$, with $0<\nu_n<2$. Although these results may, at a first glance, look confusing, we will now demonstrate that they can easily be understood, and even predicted, from a few simple principles.

To estimate the width of the linear-screening regime at small V_0 values, we follow the reasoning of Sec. II B, $V^q_{\mathrm{ext}}\approx\epsilon(q;B)V^q$, but we note that the linear approximation to the Taylor expansion of $n_{\mathrm{el}}(x)$ with respect to $V(x)$ [see Eq. (10)] no longer holds for $|V(x)|\sim 2k_BT$, since for $\nu_n\neq 1$ the second-order term $[\propto\partial^2 n_{\mathrm{el}}/\partial\mu^2=(\partial n_{\mathrm{el}}/\partial\mu)(1-\nu_n)/k_BT]$ yields already noticeable contributions for smaller $V(x)$. To take this into account, we use the linear approximation only for $|V(x)|\lesssim 2k_BT/(1+|1-\nu_n|)$ and obtain as a condition for the linear-screening regime

$$\frac{V_0}{E_F}\lesssim\frac{\epsilon(q)}{\overline{\nu}}\,\frac{\nu_n(2-\nu_n)}{1+|1-\nu_n|}. \tag{16}$$

For $\nu_n=1$ this reduces to the estimate (13). But in addition, Eq. (16) states that for even-integer filling $\nu_n\to 0$ or $\nu_n\to 2$, the linear-screening regime shrinks to zero, and it provides a good description of the widths of the linear screening regimes in the examples shown in Fig. 5.

We will now use Eq. (15) to obtain estimates of the plateau widths and heights of the Var$[V]$-vs-V_0 curves, which contain the estimate (16) for the linear-screening regime as a special case. Our estimates are based on the observation that in all cases we have studied the density modulation is nearly symmetric about the average density, so that the average of extreme values of the local filling factor is close to the average filling, $\nu(0)+\nu(a/2)\approx 2\overline{\nu}$. Nearly perfect screening occurs, if at both the potential maxima and the minima a LL is pinned to the Fermi level, so that electrons can easily be redistributed between these LL's and both $\nu(0)$ and $\nu(a/2)$ are different from even integers. If, with increasing V_0, $\nu(0)$ approaches an even-integer value $\nu(0)=2k$, the LL k is depleted at $x=0$ and a local maximum of $V(x)$ starts to develop there. Screening remains poor, and Var$[V](V_0)$ increases rapidly, until the LL $k-1$ reaches the Fermi level at $x=0$. Then a step of height $\hbar\omega_c$ is completed and the next plateau with perfect screening starts. A similar step begins as $\nu(a/2)$ reaches the value $2k'$. Then the LL $k'-1$ is completely filled at $x=a/2$ and a local potential minimum starts to develop there. Perfect screening begins again if the LL k' reaches Fermi level at $x=a/2$ and the increase of Var$[V]\times(V_0)$ by $\hbar\omega_c$ is completed.

We combine now these considerations with the estimate (15). For convenience, we introduce the dimensionless variables

$$v=\frac{V}{E_F}\quad v_0=\frac{V_0}{\epsilon(q)E_F},\quad \Omega=\frac{\hbar\omega_c}{E_F}, \tag{17}$$

and focus on the regime $0<v_0<1$, in which for $T=0$ and $B=0$ screening is linear and leads to Var$[v](v_0)=2v_0$. To keep the discussion simple, we consider the two possible cases of noninteger $\overline{\nu}=2n+\nu_n$ separately.

a. $0<\nu_n<1$. In this case the end of the linear-screening region, where $v\ll\Omega$, is reached when $\nu(0)=2n$. Then $\nu(a/2)\approx\overline{\nu}+\nu_n$ and Var$[\nu]=2\nu_n$, and across the linear-screening regime we find $\Delta\mathrm{Var}[\nu]=2\nu_n$. According to Eq. (15), linear screening ends at $V_0/E_F\sim\epsilon(q)\nu_n/\overline{\nu}$, in agreement with Eq. (16). Neglecting potential variations $\propto k_BT\ll\Omega$, we note

$$\mathrm{Var}[v]\approx 0,\quad \text{if}\quad 0<v_0<1-n\Omega, \tag{18}$$

since $\nu_n=\overline{\nu}-2n$ and $\Omega=2/\overline{\nu}$. If $n=0$, larger V_0 lead to the poor-screening quasi-1D ribbon regime.

For $n>0$, the next plateau terminates when $\nu(a/2)=2n+2$. Then $\nu(0)\approx 2n-2(1-\nu_n)$, i.e., Var$[\nu]=2(2-\nu_n)$. Across this plateau we have $\Delta\mathrm{Var}[\nu]=4(1-\nu_n)$, and with Eq. (15) $\Delta V_0\approx 2\epsilon(q)E_F(1-\nu_n)/\overline{\nu}$. This yields $\Delta v_0\approx(2n+1)\Omega-2$ and

$$\mathrm{Var}[v]\approx\Omega,\quad \text{if}\quad 1-n\Omega<v_0<(n+1)\Omega-1. \tag{19}$$

This plateau is followed by another one along which $\nu(0)$ decreases to $2(n-1)$, while $\nu(a/2)$ increases to $\approx 2n+2+2\nu_n$ and thus Var$[\nu]$ to $4+2\nu_n$. Thus, across that plateau we find $\Delta\,\mathrm{Var}[\nu]=4\nu_n$ and $\Delta v_0=2-2n\Omega$, which leads to

$$\mathrm{Var}[v]\approx 2\Omega, \quad \text{if} \quad (n+1)\Omega-1<v_0<1-(n-1)\Omega. \tag{20}$$

If $n=1$, this plateau is followed by the poor-screening quasi-1D ribbon regime. If $n>1$, we are in the same situation as at the end of the low-V_0 linear-screening regime, and a double step of total width Ω, consisting of one step of height Ω and plateau width $\Delta v_0=(2n+1)\Omega-2$ and another one of height Ω and width $\Delta v_0=2-2n\Omega$, will follow. Thus, we obtain for $0<k\leqslant n$

$$\mathrm{Var}[v]\approx(2k-1)\Omega,$$

$$\text{if} \quad 1-(n+1-k)\Omega<v_0<(n+k)\Omega-1, \tag{21}$$

$$\mathrm{Var}[v]\approx 2k\Omega, \quad \text{if} \quad (n+k)\Omega-1<v_0<1-(n-k)\Omega. \tag{22}$$

Thus, the linear screening regime is followed by n double steps, which sum up to a total width $\Delta v_0=1$, and on the last plateau (before breakdown) we have $\mathrm{Var}[v]=2(1-\nu_n/\bar{\nu})$. For $0<\nu_n<0.5$, the first plateau of the double step is wider than the second one, as for the dash-dotted line in Fig. 5 ($\bar{\nu}=2.33$), while for $0.5<\nu_n<1$ the second plateau of the double step is the wider one, as for the short-dashed line ($\bar{\nu}=2.67$).

We should mention three limits. For $\nu_n\to 0$ the low-V_0 linear-screening regime shrinks to zero and the first plateau of the double step exhausts its full width, so that the second step merges with the first one of the following double step. Thus, we observe at small V_0 a step of height Ω, followed by steps of the double height 2Ω, and all plateaus have the same widths, as we found previously. For $\nu_n=0.5$ we get an even number of steps which all have the same heights and widths. For $\nu_n\to 1$ the width of the first plateau of each double step shrinks to zero, so that the low-V_0 linear-screening regime is followed by steps of height 2Ω and width Ω, as we have seen before.

b. $1<\nu_n<2$. In this case we have at the end of the linear screening regime $\nu(a/2)=2n+2$ and $\nu(0)\approx 2n+2(\nu_n-1)>2n$, with $\mathrm{Var}[\nu]=2(2-\nu_n)$. From Eq. (15) we obtain

$$\mathrm{Var}[v]\approx 0, \quad \text{if} \quad 0<v_0<(n+1)\Omega-1, \tag{23}$$

and see that now the linear screening regime is always followed by a step of height Ω to a plateau of perfect screening. For $n=0$ (i.e., $1<\Omega<2$) this plateau covers the interval $\Omega-1<v_0<1$ (see, e.g., thin dashed line of Fig. 5 for $\bar{\nu}=1.33$). To estimate for $n>0$ height and width of the following steps and plateaus, respectively, we proceed as before, exploiting that at the end of each plateau either $\nu(0)$ or $\nu(a/2)$ reaches an even integer value and that $\nu(0)+\nu(a/2)\approx 2\bar{\nu}$. The result is, for $0<k\leqslant n$, a double step of total width Ω,

$$\mathrm{Var}[v]\approx(2k-1)\Omega,$$

$$\text{if} \quad (n+k)\Omega-1<v_0<1-(n+1-k)\Omega, \tag{24}$$

$$\mathrm{Var}[v]\approx 2k\Omega,$$

$$\text{if} \quad 1-(n+1-k)\Omega<v_0<(n+k+1)\Omega-1, \tag{25}$$

which is followed by a final single step

$$\mathrm{Var}[v]\approx(2n+1)\Omega, \quad \text{if} \quad (2n+1)\Omega-1<v_0<1, \tag{26}$$

of height Ω and plateau width $2-(2n+1)\Omega$. The linear-screening regime [width $(n+1)\Omega-1$], the n double steps, and this final plateau cover together the interval $0<v_0<1$, as in the case $0<\nu_n<1$. The variance of the screened potential in the last plateau is $\mathrm{Var}[v]=2[1-(\nu_n-1)/\bar{\nu}]$.

For $1<\nu_n<1.5$ the first plateau of each double step is wider than the other plateaus, as seen in Fig. 5 for the long-dashed line ($\bar{\nu}=3.25$), which exhibits one double step following the initial single step. For $1.5<\nu_n<2$ these first plateaus are the narrower ones, as seen for the thick solid line ($\bar{\nu}=3.75$). For $\nu_n=1.5$, the double steps consist of two individual steps of equal heights and plateau widths, as is illustrated by the thin solid line ($\bar{\nu}=7.5$).

In the limit of odd-integer $\bar{\nu}$, $\nu_n\to 1$, the width of the first single step together with the second plateau width of each double step shrinks to zero, so that only steps with step height 2Ω and plateau width Ω occur. (For $\bar{\nu}=1$, i.e., $n=0$, no double step exists and the single step merges with the breakdown regime.) In the even-$\bar{\nu}$ limit, $\nu_n\to 2$, the width of the first plateau of each double step shrinks to zero. Thus, the first step of width Ω and height Ω is followed by n steps of the same plateau width but double step height.

c. *Summary.* Summarizing the estimates of this Sec. II C, we note that the Eqs. (18)–(26) define a set of straight lines in the v_0-Ω plane, which separate areas in each of which the variance $\mathrm{Var}[v](v_0)$ equals an integer multiple of Ω. This is schematically shown in Fig. 6. The position and height of the steps of the $\mathrm{Var}[v](v_0)$ curve for a given value of $\bar{\nu}$ can immediately be read off from this figure along the vertical line at $\Omega=2/\bar{\nu}$.

D. Sweeping the magnetic field

We now consider the screening of an external cosine potential $V_{\mathrm{ext}}(x)=V_0\cos qx$ of fixed amplitude V_0 as function of the magnetic field B, keeping the average electron density at the fixed value of the positive background charge density. Then, with increasing B the average filling factor $\bar{\nu}=2E_F/\hbar\omega_c$ decreases. For the unmodulated 2DEG ($V_0=0$), this leads to the well-known sawtooth behavior of the chemical potential, which at low temperatures is pinned to the LL's, i.e. follows half-integer multiples of the cyclotron energy,

$$\mu^\star=\hbar\omega_c(n+1/2) \quad \text{if} \quad 1/(n+1)<\Omega<1/n. \tag{27}$$

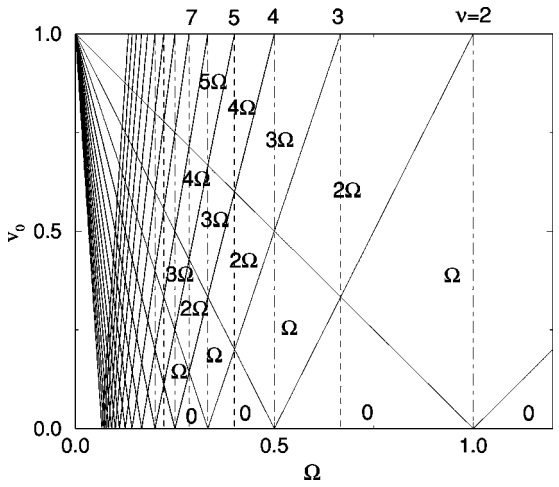

FIG. 6. The solid lines indicate $v_0=k\Omega-1$ and $v_0=1-k\Omega$ for $v_0=V_0/[E_F\epsilon(q)]$, $\Omega=\hbar\omega_c/E_F$, and $k=1,2,\ldots,15$. Even- (odd-) integer values of the average filling factor are indicated by dash-dotted (dashed) vertical lines. Within each area defined by the solid lines the value of $\mathrm{Var}[V]/E_F$ equals an integer multiple of Ω. This value increases by Ω if a solid line is crossed in the upward direction. The region $v_0>1$ corresponds to the poor-screening regime of parallel, disconnected, quasi-1D electron systems.

In the modulated 2DEG ($V_0>0$), pinning of LL's to the electrochemical potential causes the total variance of the screened potential to be an integer multiple of the cyclotron energy. Thus, for the variance $\mathrm{Var}[V]$ as function of B we expect a similar sawtooth behavior as for the $\mu^\star$-vs-B curve. Numerical results for several values of V_0 are shown in Fig. 7. The uppermost curve for the largest modulation amplitude looks indeed similar to a $\mu^\star$-vs-B curve. However, whereas the latter with decreasing B always jumps to the next higher LL, the $\mathrm{Var}[V]$-vs-B curves can also jump back to the next lower LL, as is more clearly seen for the curves with smaller modulation amplitudes. This seemingly irregular behavior of the $\mathrm{Var}[V](\Omega)$ curves in Fig. 7 can easily be understood from Fig. 6, where we now have to follow horizontal lines.

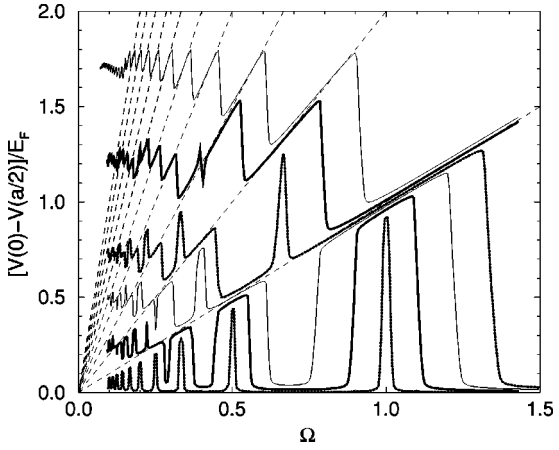

FIG. 7. Variance of the screened potential vs $\Omega_c=\hbar\omega_c/E_F$ for $V_0/E_F=1,5,10,15,25,35$ (from bottom to top). The straight dashed lines indicate integer multiples of the cyclotron energy [$k_BT/E_F=0.01$, $\epsilon(q)=41$].

For fixed $v_0^0=V_0/[E_F\epsilon(q)]$ and decreasing Ω, the variance $\mathrm{Var}[V]/E_F$ increases by Ω if the horizontal line $v_0=v_0^0$ intersects one of the straight lines $v_0=k\Omega-1$ and decreases by Ω if it intersects one of the straight lines $v_0=1-k\Omega$. For large V_0 ($v_0>0.6$), the variance jumps with decreasing B monotonically to higher multiples of the cyclotron energy, until B becomes so small that $\Omega=1-v_0^0$. Then, for smaller B also jumps back to lower multiples occur. For small modulation amplitude ($v_0^0\lesssim 0.1$) one has perfect screening if the average filling factor is not too close to an even integer. Near such values linear screening breaks down and $\mathrm{Var}[V]/E_F$ approaches Ω, provided $2V_0>\hbar\omega_c$ (otherwise $\mathrm{Var}[V]=2V_0$). For sufficiently small B, of course, the variance will equal higher multiples of the cyclotron energy, so that the correct linear-screening limit is obtained in the limit of zero magnetic field. Thus, if one adds the smoothing effect of finite temperature, one can understand all properties of the apparently irregular $\mathrm{Var}[V](\Omega)$ traces in Fig. 7 in terms of the peculiar but regular v_0-vs-Ω pattern sketched in Fig. 6.

III. HALL-BAR GEOMETRY

A. Boundary conditions and kernels

We now consider a 2DEG with lateral confinement in the x direction and translation invariance in the y direction, i.e., an idealized Hall-bar geometry. To study boundary effects on the screening properties, we will apply an additional periodic external modulation potential in x direction. We will consider two different sets of boundary conditions, which lead to slightly different confinement potentials.

1. In-plane gates

Following Refs. 10–13 we first assume that all charges reside in the plane $z=0$ and that the half-planes $z=0$, $x<-d$ and $z=0$, $x>d$ are kept at constant electrostatic potential, $V(x,y,z=0)=0$ for $|x|>d$ (in-plane gates).[11,13] Then the electrostatics can be solved using the theory of complex functions, and the kernel in Eq. (1), with $-x_l=x_r=d$, is obtained as[13]

$$K_\parallel(x,t)=\ln\left|\frac{\sqrt{(d^2-x^2)(d^2-t^2)}+d^2-tx}{(x-t)d}\right|. \qquad (28)$$

Positive background charges of the 2D charge density en_0 between the in-plane gates will produce the confinement potential (written as potential energy of an electron)

$$V_{\mathrm{bg}}(x)=-E_0\sqrt{1-(x/d)^2},\quad E_0=2\pi e^2 n_0 d/\overline{\kappa}, \qquad (29)$$

which can be calculated from Eq. (1) using the kernel (28) and replacing $n_{\mathrm{el}}(x')$ by $-n_0$.

2. Perpendicular gates

Another simple set of boundary conditions is obtained assuming the 2DEG to be laterally confined by two equipotential planes located at $x=\pm d$ parallel to the y-z plane, $V(x=\pm d,y,z)=0$. This is a reasonable model for a free-standing mesa-etched Hall bar with free or metallized sur-

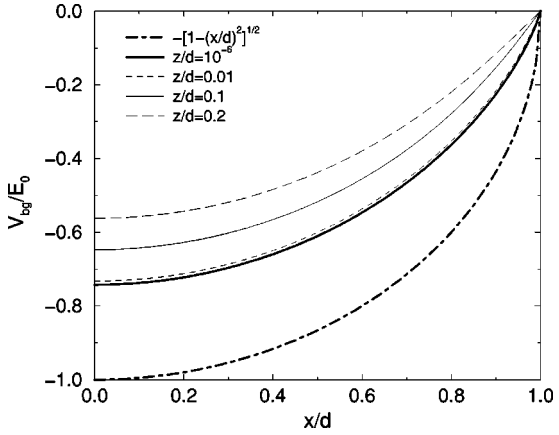

FIG. 8. Confinement potential $V_{\rm bg}(x,y,z=0)/E_0$ due to a homogeneous plane of charge density en_0 at distance z. The dash-dotted line is obtained from model (28) with $z=0$; the other lines are for model (30).

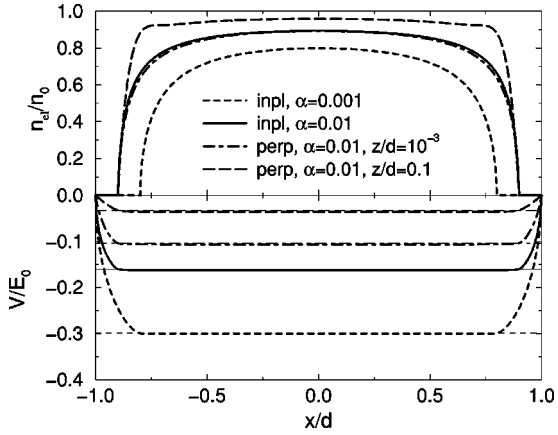

FIG. 9. Some consistent density profiles (upper panel) and potentials (lower panel) calculated for the in-plane-gate model (28) and the perpendicular-gate model (30), respectively. The depletion length is chosen as $d/5$ for the short-dashed curves and as $d/10$ otherwise. Thin horizontal lines indicate the corresponding electrochemical potentials. $\alpha=\pi a_B^\star/2d$, $T=0$, $B=0$.

faces at $x=\pm d$, which accommodate a large number of (partially occupied) surface states. The electrostatics with these boundary conditions is well known.[15] In our notation it is expressed by the kernel

$$K_\perp(x,t)=-\ln\left(\frac{\cos^2\dfrac{\pi}{4d}(x+t)+\gamma^2}{\sin^2\dfrac{\pi}{4d}(x-t)+\gamma^2}\right) \tag{30}$$

for $\gamma\to 0$. Inserting this with $\gamma=\sinh(\pi z/4d)$ into Eq. (1), where $-x_l=x_r=d$, yields the electrostatic potential $V_H(x,y,z)$ due to the 2DEG at a position separated by the distance $|z|$ from the plane of the 2DEG. Correspondingly, we can use this to calculate the confinement potential produced in the plane of the 2DEG by a plane, positive background charge at a distance z from the 2DEG. Typical confinement potentials are shown in Fig. 8. For $\gamma=0$ the potential minimum is $V_{\rm bg}(0,y,0)/E_0=-8G/\pi^2=-0.742\,46$, with Catalan's constant[18] $G=0.915\,965\,594$.

The positive background charge density and sample width define the characteristic energy E_0, Eq. (29). Measuring energies in units of E_0, lengths in units of d, and density of states in units of D_0, we obtain from Eq. (2) the dimensionless electron density $\tilde{n}(x/d)=n_{\rm el}(x)/E_0D_0$, so that Eq. (1) assumes a dimensionless form with the prefactor $1/\alpha_{\rm conf}$, where

$$\alpha_{\rm conf}=\pi a_B^\star/2d \tag{31}$$

measures the relative strength of the Coulomb interaction, similar to α of Eq. (9). We will usually assume $\alpha_{\rm conf}=0.01$, i.e., for GaAs, a sample width $2d\sim 3$ μm, since this allows us to calculate density profiles with clearly visible incompressible strips on a mesh of relatively few (~ 500) points across the sample. For much larger d, we would need a much finer mesh, i.e., more ambitious numerics, and the incompressible strips would be hardly visible on that scale, although the physics would not change qualitatively.

Figure 9 shows some density and potential profiles obtained for the two sets of boundary conditions in the limit of zero temperature and magnetic field, where $n_{\rm el}(x)/n_0=(\pi/\alpha_{\rm conf})\mu(x)\,\theta(\mu(x))/E_0$, with $\mu(x)=\mu^\star-V(x)$. Apparently the density profiles are very similar if we assume the same depletion length, the same sample width, and vanishing spacer between 2DEG and background charges (i.e., $z=0$) in both cases.

B. Unmodulated system in a magnetic field

In the ideal homogeneous 2DEG at low temperatures, the chemical potential as a function of magnetic field exhibits the well-known sawtooth behavior, Eq. (27). With decreasing B it follows a Landau energy $(n+1/2)\hbar\omega_c$ until the filling factor $\nu=2E_F/\hbar\omega_c$ reaches the value $2(n+1)$, and then it jumps to the next higher LL. In the confined system, the self-consistently calculated "chemical potential" $\mu(0)=\mu^\star-V(0)$ in the center, $x=0$, shows the same behavior, as is seen in Fig. 10(c), where $\mu(x=0;B,T)$ in units of $\mu_0\equiv\mu(x=0;0,0)$ is plotted as function of $\Omega=\hbar\omega_c/\mu_0$.

However, in contrast to the chemical potential oscillations in a homogeneous 2DEG, the corresponding oscillations in the confined system are realized by strong spatial variations of the electrostatic potential in the interior of the sample. This is demonstrated in Fig. 10(b), which shows the self-consistent total potential in the interior of the sample for the four values of Ω indicated by open circles in Fig. 10(c). Figure 10(a) shows the corresponding density profiles, normalized as the local filling factor, $\nu(x)=2\pi l^2 n_{\rm el}(x)$. For $\nu(x)\leqslant\nu(0)\approx 2/\Omega<2$ the LL $n=0$ is pinned to the electrochemical potential $\mu^\star$ nearly everywhere in the 2DEG. For $\nu(0)\gtrsim 2$ the LL $n=1$ must be partially populated in the center of the sample. This forces the potential to develop a local minimum near the center, with a decrease of $V(0)$ by an amount $\sim\hbar\omega_c$, so that a compressible strip starts to develop in the center. With further increasing $\nu(0)$, this central compressible strip becomes broader and the adjacent incom-

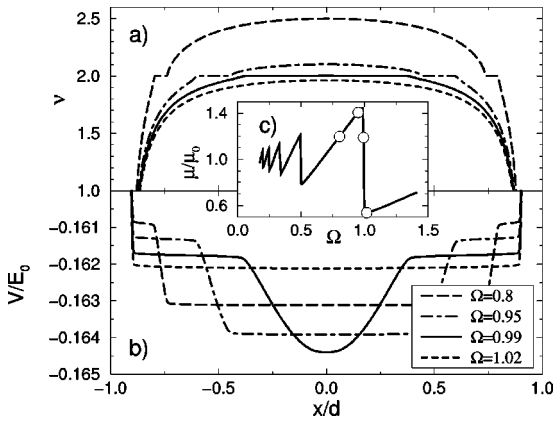

FIG. 10. (a) Filling factor $\nu(x)$ and (b) potential $V(x)$ for the values of $\Omega=\hbar\omega_c/\mu_0$ given in the legend and indicated by open circles in (c), which shows the "chemical potential" $\mu=\mu^\star-V(0)$, calculated with model (28) for parameter values $\pi a_B^\star/2d=0.01$, $\mu_0/E_0=0.002\,84$, $k_BT/E_0=2\times10^{-5}$.

pressible strips, together with the related potential steps, move towards the sample edges. Similar drastic changes of the potential distribution are found near all jumps of the chemical potential. Thus, pinning and screening lead already to drastic effects in the confined 2DEG even in the absence of any additional potential modulation.

C. Confined system with modulation

We now add a symmetric external modulation potential to the confinement potential and investigate how this affects the self-consistent potential. We take $V_{\rm ext}(x)=V_0\cos(2.5\pi x/d)$ which is in accordance with our general boundary conditions and exhibits just one full oscillation period in the interior of the sample, so that we can expect similar screening effects, as in a homogeneous unbounded system, and possibly some effects of the nearby sample edges. The period of this modulation is $a=2d/2.5$, so that the choice $\alpha_{\rm conf}=0.01$ implies $\alpha=1/40$ [see Eq. (9)] and the results can be compared immediately with the previous one for the unbounded 2DEG. For this comparison it will be important whether the potential of the unmodulated system has a strong variation in the center region or not, i.e., whether the filling factor $\nu(0)$ in the center is slightly larger than an even integer or not.

1. Weak boundary effects on screening

To describe the screening of an external modulation potential, it seems natural to calculate the difference $\Delta V(x;V_0)=V(x;V_0)-V(x;0)$ of the self-consistent potentials with and without the modulation. If $V(x;0)$ is flat in the interior of the sample, we expect that screening is very similar to that in an unconfined system and that $\Delta V(x;V_0)$ contains essentially the same information as $V(x;V_0)$, apart from an unimportant constant offset. This is indeed true if $\nu(0)$ is not closely above an even integer. As an example, we compare in Fig. 11 numerical results for the two confinement models and for the unconfined 2DEG. The results for the density of the confined 2DEG differ only slightly in the edge regions. In the interior, the filling factors $\nu(x)$ are practically

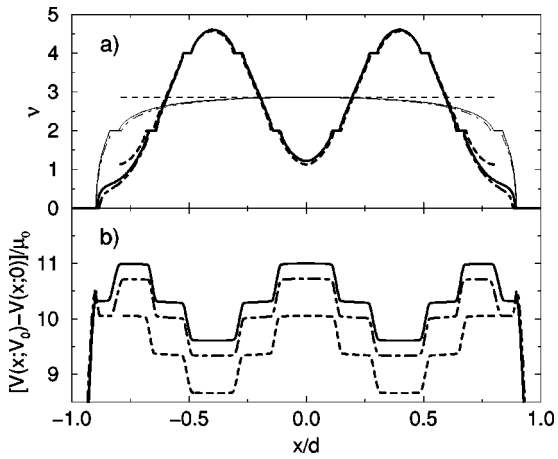

FIG. 11. (a) Filling factor $\nu(x)$ and (b) screened potential $\Delta V(x;V_0)$ for the confinement models (28) (solid lines) and (30) (dash-dotted lines) and for the unconfined 2DEG (dashed lines). Thin lines show $\nu(x)$ without modulation, with $\nu(0)=2.8574$ for all models. The screened potential for the unbounded 2DEG is shifted by a constant and actually oscillates symmetrically around zero ($\alpha_{\rm conf}=0.01$, $\mu_0/E_0=0.002\,842$, $\hbar\omega_c/\mu_0=0.7$, $V_0/\mu_0=24.63$, $k_BT/\mu_0=0.007$).

the same and agree well with that of the unconfined 2DEG with the same modulation potential. Also the screened potentials are equivalent and differ only by a constant offset, which results from the asymmetry of the density modulation with respect to the unmodulated electron density profile.

2. Strong confinement effect on screening

Things become more complicated if already without additional external modulation the potential near the center of the Hall bar varies strongly, as happens for $\nu(0)=2n+\nu_n$ with $0<\nu_n\ll1$. Then, for small modulation amplitude ($V_0\ll\hbar\omega_c$), the self-consistent potential $V(x;V_0)$ follows $V(x;0)$, with a minimum at $x=0$, and only the difference $\Delta V(x;V_0)$ reminds us of an oscillatory potential with the phase of the external modulation; see solid lines in Fig. 12. For stronger modulation ($V_0\lesssim\hbar\omega_c$), $V(x;V_0)$ develops a local maximum at $x=0$ and the total variation of $V(x;V_0)$ in the center region $|x|\lesssim d/2$ is of the order of $V_0<\hbar\omega_c$; see Fig. 12(a). The variation of $\Delta V(x;V_0)$ is now, however, by an amount of $\hbar\omega_c$ larger. In this small-V_0 regime screening is rather poor and very nonlinear. As V_0 increases further, the variance $\mathrm{Var}[V](V_0)=V(0;V_0)-V(a/2;V_0)$ (note that $a/2=0.4d$) approaches the plateau value $\hbar\omega_c$ and then behaves as a function of V_0 just as for the unconfined 2DEG. The variance of the "screened potential" $\Delta V(x;V_0)$, on the other hand, will be by about $\hbar\omega_c$ larger in the plateau region.

To summarize, if we neglect the relatively narrow V_0 interval between the plateaus, we find that the variance of the self-consistent potential $V(x;V_0)$ as a function of V_0 shows the same behavior as for the unconfined 2DEG. For most magnetic field values, the variance of the "screened potential" $\Delta V(x;V_0)$ also shows the same characteristics. Only if the filling factor $\nu(0)$ in the center of the unmodulated confined 2DEG is slightly larger than an even integer does the

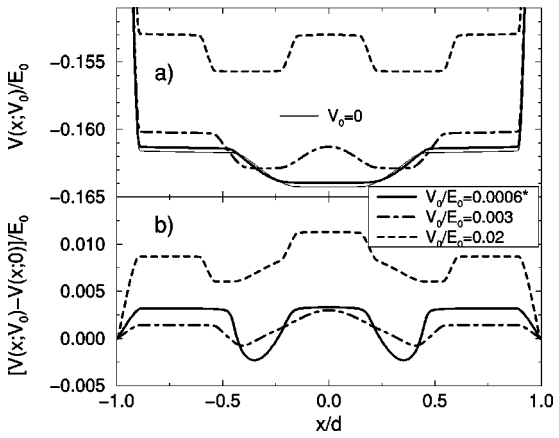

FIG. 12. (a) Self-consistent potential $V(x;V_0)$ and (b) screened potential $\Delta V(x;V_0)$, for several V_0. For clarity, (b) shows $10\Delta V(x;V_0)$ for the weakest modulation $V_0=6\times10^{-4}E_0$. For $V_0=0$ [thin solid line in (a)] $\nu(0)=2.03$ ($\alpha_{\rm conf}=0.01$, $\mu_0/E_0=0.002842$, $\hbar\omega_c/\mu_0=0.985$, $k_BT/\mu_0=0.01$).

spatial variation of the self-consistent potential $V(x;0)$ of the unmodulated system cause the variance of $\Delta V(x;V_0)$ to be about $\hbar\omega_c$ larger than the variance of $V(x;V_0)$. If we plot the variance of $\Delta V(x;V_0)$ at fixed V_0 as a function of $\Omega=\hbar\omega_c/\mu_0$, we get sawtoothlike traces as in Fig. 7, however with additional spikes of height Ω at $\Omega\lesssim1/k$ for integer k.

IV. SUMMARY

We have investigated the screening of a harmonic external potential by an unconfined two-dimensional electron gas as well as by confined 2DEG's in a simplified Hall geometry, in strong perpendicular magnetic fields, and at low temperatures. Our numerical results within the self-consistent Thomas-Fermi-Poisson approach show that screening is very nonlinear and dominated by the phenomenon of pinning of Landau levels to the electrochemical potential, which leads to compressible regions with position-dependent electron density, where this pinning takes place, and to incompressible regions of constant density and position-dependent electrostatic potential in between. At fixed magnetic field, the total variation (''variance'' Var$[V]$) of the self-consistently calculated potential energy increases with increasing modulation amplitude V_0 in a steplike fashion, exhibiting plateaus, where the value of Var$[V]$ is close to an integer multiple of the cyclotron energy and shows a weak linear increase with V_0, with a slope proportional to the temperature. The corresponding modulation of the electron density is, in contrast to the potential, not strongly affected by the magnetic B. The occurrence of incompressible strips leads to local modifications, but the overall density profile is roughly the same as for $B=0$, as has already been emphasized by Chklovskii *et al.*[10] Exploiting this observation together with the pinning phenomenon and the relations between density modulation and external and screened potential valid in the linear-screening regime, we were able to derive simple analytical expressions for step heights and plateau widths of the Var$[V]$-vs-V_0 curves for arbitrary B and $T=0$. This simple analytical description of nonlinear screening in an unconfined 2DEG is summarized in Fig. 6 and allows also an easy understanding of the complicated traces obtained while plotting Var$[V]$ as a function of B at fixed V_0 (see Fig. 7).

Finally we have investigated the corresponding screening properties of a confined 2DEG in a simplified Hall geometry for two different types of boundary conditions, which lead to different confinement potentials, but nearly identical density profiles, apart from slight deviations in the edge regions. Considering the effect of an external modulation potential $V_{\rm ext}(x)=V_0\cos(2.5\pi x/a)$ in the interior of the sample (more than about $a/2$ from the edges), we find essentially the same properties as for the unbounded 2DEG. Care must be taken, however, if in the center of the unmodulated system a new Landau level starts to be occupied, since then the self-consistent potential varies strongly in the center region. This is an interesting confinement effect, but it can be easily eliminated from the discussion of screening if the modulation amplitude V_0 is large enough.

ACKNOWLEDGMENTS

We gratefully acknowledge stimulating discussions with E. Ahlswede and K. Muraki as well as financial support by the Deutsche Forschungsgemeinschaft, SP ''Quanten-Hall-Systeme'' Grant No. GE306/4-2.

[1] U. Wulf, V. Gudmundsson, and R.R. Gerhardts, Phys. Rev. B **38**, 4218 (1988).
[2] A.L. Efros, Solid State Commun. **67**, 1019 (1988).
[3] A.L. Efros, F.G. Pikus, and V.G. Burnett, Phys. Rev. B **47**, 2233 (1993).
[4] V.G. Burnett, A.L. Efros, and F.G. Pikus, Phys. Rev. B **48**, 14 365 (1993).
[5] N.R. Cooper and J.T. Chalker, Phys. Rev. B **48**, 4530 (1993).
[6] V. Tsemekhman, K. Tsemekhman, C. Wexler, J.H. Han, and D.J. Thouless, Phys. Rev. B **55**, R10 201 (1997).
[7] K. Güven, R.R. Gerhardts, I.I. Kaya, B.E. Sagol, and G. Nachtwei, Phys. Rev. B **65**, 155316 (2002).
[8] I.I. Kaya, G. Nachtwei, K. von Klitzing, and K. Eberl, Europhys. Lett. **46**, 62 (1999); Phys. Rev. B **58**, R7536 (1998).
[9] I.I. Kaya, G. Nachtwei, B.E. Sagol, K. von Klitzing, and K. Eberl, Physica E (Amsterdam) **6**, 128 (2000).
[10] D.B. Chklovskii, B.I. Shklovskii, and L.I. Glazman, Phys. Rev. B **46**, 4026 (1992).
[11] D.B. Chklovskii, K.A. Matveev, and B.I. Shklovskii, Phys. Rev. B **47**, 12 605 (1993).
[12] K. Lier and R.R. Gerhardts, Phys. Rev. B **50**, 7757 (1994).
[13] J.H. Oh and R.R. Gerhardts, Phys. Rev. B **56**, 13 519 (1997).
[14] T. Ando, A.B. Fowler, and F. Stern, Rev. Mod. Phys. **54**, 437 (1982).

[15] P.M. Morse and H. Feshbach, *Methods of Theoretical Physics* (McGraw-Hill, New York, 1953), Vol. II, p. 1240.
[16] F. Stern, Phys. Rev. Lett. **18**, 546 (1967).
[17] U. Wulf and R.R. Gerhardts, in *Physics and Technology of Submicron Structures*, Vol. 83 of *Springer Series in Solid-State Sciences*, edited by H. Heinrich, G. Bauer, and F. Kuchar (Springer-Verlag, Berlin, 1988), p. 162.
[18] I.S. Gradshteyn and I.M. Ryzhik, *Table of Integrals, Series, and Products* (Academic Press, New York, 1994).